



“Babeş-Bolyai” University of Cluj-Napoca
Faculty of Chemistry and Chemical Engineering



PhD thesis

Electrodes modified with nanomaterials for biomedical applications and environmental protection

-Abstract -

Scientific advisor,

Prof. Dr. Liana Maria MUREŞAN

PhD student,

Aglaia Raluca DEAC

Cluj Napoca

2017

“Babeş-Bolyai” University of Cluj-Napoca
Faculty of Chemistry and Chemical Engineering

Aglaia Raluca DEAC

Electrodes modified with nanomaterials for biomedical applications and environmental protection

-Abstract-

Jury:

President:

Prof. Dr. Tiberiu FRENTIU

“Babeş-Bolyai” University of Cluj-Napoca
Faculty of Chemistry and Chemical Engineering

Scientific advisor:

Prof. Dr. Liana Maria Mureşan

“Babeş-Bolyai” University of Cluj-Napoca
Faculty of Chemistry and Chemical Engineering

Reviewers:

Prof. Dr. Robert Sandulescu

UMF Cluj Napoca

Prof. Dr. Ing. Nicolae Vaszilcsin

Polytechnic University of Timișoara

Conf. Dr. Ing. Graziella Turdean

“Babeş-Bolyai” University of Cluj-Napoca

Faculty of Chemistry and Chemical Engineering

Table of contents

Introduction	10
Objectives of the thesis	14
Part I Literature study	
Chapter 1 Carbon Xerogels	16
1.1. General Aspects	16
1.2. Sol-Gel synthesis method of nanomaterials	19
1.3. Doping: The process of improving the properties of xerogels	27
1.4. Properties of xerogels	28
1.5. Applications of carbon xerogels	30
1.6. Electrodes modified with carbon xerogels:	32
1.6.1 Obtaining modified electrode materials	32
1.6.2 Conductive ink based on xerogels doped with metals	34
1.7. Methods of Characterization of Modified Electrodes	40
1.7.1. Electrochemical methods	41
1.7.1.1 Cyclic voltammetry	40
1.7.1.2 Square wave stripping voltammetry	43
1.7.1.3 Electrochemical Impedance Spectroscopy	44
1.7.2. Methods of morpho-structural analysis	46
1.7.2.1. Scanning Electron Microscopy (SEM)	46
1.7.2.2. Electronic transmission microscopy (TEM)	47
1.7.3. Dynamic Light Scattering (DLS)	49
1.7.4. Viscosity measurement	51
1.7.5. Surface tension measurement	52
1.8. Conclusions	53
Capitolul 2. Hemin modified electrodes for H ₂ O ₂ detection	54
2.1. Hemine-pseudo-enzymatic catalyst	54
2.2. Electrodes modified with graphene and hemin	56
2.2.1 Graphene: General Aspects	56
2.2.2 Preparation method	59

2.2.3	Graphene properties	61
2.2.4	Graphene applications	62
2.2.5	Electrodes modified with graphene oxide and hemin	63
2.3	Electrodes modified with melaminic compounds and hemin	64
2.3.1	Dendrimers: General aspects	64
2.3.2	Melaminic dendrimers	67
2.3.3	Electrodes modified with dendrimers	69
2.4	Conclusions	72
Part a-2-a Personal contributions		
Capitolul 3.	Electrodes modified with carbon xerogels doped with Bi	74
3.1.	Synthesis of electrode materials	74
3.2.	Morpho-structural characterization of BiCXe-CPE	76
3.3.	Carbon paste electrodes for detection of Cd ²⁺ și Pb ²⁺ ions:	77
3.3.1.	Electrode preparation BiCXe-CPE	77
3.3.2.	Electrochemical characterization of BiCXe-CPE through cyclic voltammetry and square wave voltammetry	79
3.3.3.	Cd ²⁺ ions detection	83
3.3.4.	Interference studies	86
3.3.5.	Pb ²⁺ ions detection	88
3.4.	Conclusions	93
Capitolul 4.	Screen-printed electrodes based on carbon xerogels doped with Bi	94
4.1	Conductive ink preparation	94
4.2	Ink characterization	98
4.3	Tests on photographic paper	106
4.4	Preliminary electrochemical tests	107
4.5	Conclusions	107
Capitolul 5.	Modified electrodes based on hemin for H ₂ O ₂ detection	109
5.1	Modified electrodes based on graphene and hemin	110
5.1.1	Electrodes preparation	111
5.1.2	Modified electrodes characterization	113
5.1.3	H ₂ O ₂ determination with G/rGO/polyHm modified electrodes	123

5.1.3.1 Determination of H ₂ O ₂ concentration in a real sample	127
5.2. Conclusions	128
5.3. Electrodes modified with melaminic compounds and hemin	128
5.3.1 Experimental conditions	128
5.3.2 Electrodes modified preparation	130
5.3.3 Methods for characterization of modified electrodes	131
5.3.3.1 FT-IR analysis	131
5.3.3.2 Electrochemical methods	133
5.3.4 Amperometric detection of H ₂ O ₂	140
5.4. Conclusions	144
6. Conclusions and perspectives	145
7. Bibliography	147
8. Scientific activity	164

Keywords: modified electrodes; sol-gel process; xerogel carbon doped with bismuth; heavy metals; reduction of hydrogen peroxide; hemin; melamine compounds; graphene.

Introduction

Detection of heavy metal ions is of particular importance due their toxicity, negative impact on environmental quality and increased presence [Wang J., 2005]. In this context, it is necessary to develop new cheap and effective tools and methods for the rapid evaluation of heavy metals traces from different systems [Aragay G., Merkoci A., 2012], [Wang J., 2005] [Rodrigues JA, et al., 2011].

Another problem approached and developed in this thesis is amperometric detection of hydrogen peroxide using hemin-based electrodes.

Shortly, the originality of this research consists in the preparation and electrochemical testing of new modified electrodes based on: (i) bismuth doped carbon xerogels for the detection of heavy metals such as Cd^{2+} and Pb^{2+} from aqueous solutions as an ecological and cheaper alternative to Hg electrodes; (ii) graphene and hemine; (iii) hemine and melamine compounds, in order to prepare sensible devices for H_2O_2 detection.

The paper is structured in two parts. The first part is named "Literature Study" and contains 2 chapters as follows.

Chapter 1 "Modified electrodes based on carbon Xerogels" presents the most important bibliographic data in relation to these materials in a specific approach.

The second chapter, entitled "Electrodes modified with hemin for detection of H_2O_2 " also includes two subchapters: (i) "modified electrodes based on graphene and hemine" and the second subchapter, "Modified electrodes based on melamine compounds and hemin". This section presents the introductive notions about the pseudo-enzymatic catalyst specified in the title of the chapter, used for the detection of hydrogen peroxide, addresses general notions about graphene - innovative materials, about melamine compounds, as well as the latest news regarding electrodes modified with these materials.

Part 2, entitled Personal contributions presents the original research undertaken in doctoral years and is also structured in three chapters.

Chapter 3 of the thesis, entitled "Bi-doped carbon-modified carbon electrodes", presents the experimental results obtained with doped / undoped carbon xerogel as a modifier for the construction of sensors with applications in heavy metal detection, and Chapter 4 shows the results obtained with the material used in the previous chapter tested in another form, as conductive ink. Research on this subject is at the outset and the ideas will materialize in the near future, along with the team of researchers at the Barcelona Institute of Materials Science (ICMAB).

Chapter 5, entitled "Hemin-modified electrodes for H₂O₂ detection" is divided into two sub-chapters: (i) "Graphene-modified electrodes" and (ii) "Melamine-modified electrodes". Both chapters refer to the three types of electrodes over which we worked during the research, providing a broad overview of laboratory methodology, data processing and a synthesis of the obtained results.

The thesis ends with the presentation of the general conclusions, followed by the perspectives and the scientific activity of the undersigned.

The results obtained are only an introduction to the study of these materials of electrochemical interest, a study that needs to be continued and deepened to broaden the area of knowledge of both experimental research and theoretical development. Another purpose of this thesis is to present the perspectives which these materials can achieve and what they can offer as novelties in the electrochemistry of materials.

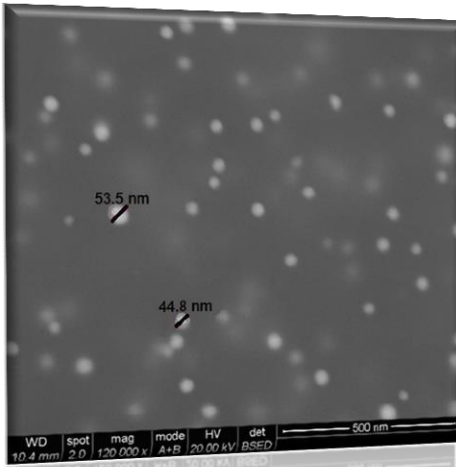
This thesis is a multidisciplinary approach to nanomaterials, morpho-structural investigation techniques and sensors with a high potential for environmental and health protection. This puts our country in a new research direction of European interest: replacing the mercury electrode for sensory applications with non-toxic composite materials based on bismuth [Svancara I, 2010], as well as making sensors for the detection of hydrogen peroxide, which is a key compound in medicine, in oxidative therapies, detoxification of the body, etc.

Chapter 3. Modified electrodes with carbon xerogel doped with Bi

3.1. Synthesis of electrode materials

The process of obtaining doped carbon xerogels through sol-gel process includes: sol preparation, a process based on the polycondensation reaction of resorcinol with formaldehyde (F) in the presence of basic catalyst NH_4OH and formal glycerol, and sol maturation (gelling) at 60°C in an oven for 3 days in hermetically sealed glass containers. This process is followed by doping the resulting RF gel with the Bi^{3+} salt; washing the gel in acetic acid; drying under ambient conditions (at room temperature) and heat treatment by pyrolysis ($550^\circ\text{C} / 2\text{h} / \text{Ar}$ - in inert atmosphere).

3.2. Morpho-structural characterization



SEM investigations performed on doped carbon xerogel (BiCXe) reveal the presence of spherical bismuth nanoparticles with a mean diameter of about 50 nm, evenly dispersed in the porous material structure (Figure 3.2).

Figure 3.2. The SEM image of the bismuth-doped carbon xerogel (BiCXe-CPE)

3.3. Carbon paste electrode for Cd^{2+} and Pb^{2+} ion detection

3.3.1. Preparation of the BiCXe-CPE electrode

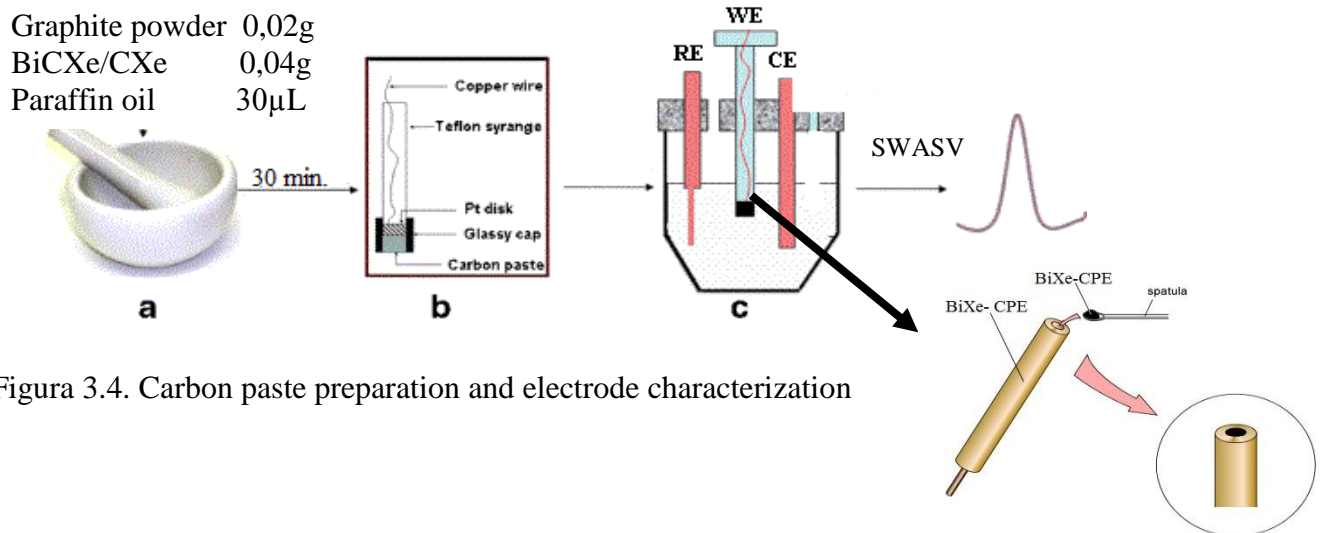


Figure 3.4. Carbon paste preparation and electrode characterization

Both modified electrodes with CXe-CPE (blank) and BiCXe-CPE bismuth doped carbon paste were prepared as follows: graphite powder (0.02 g), CXe or BiCXe-CPE (0.04 g) and paraffin oil (30 μ L) were carefully mixed in a mortar, until complete homogenization, for 30 minutes. The pastes obtained were placed in a cylindrical support; the surface of the electrode being thus polished on a white paper, and renewed with a fresh one after each experiment. The electrode thus obtained was used without any chemical or electrochemical pretreatment.

3.3.2. Electrochemical characterization of the BiCXe-CPE electrode by cyclic and square wave voltammetry

Cyclic voltammograms recorded for the BiCXe-CPE electrode compared to those obtained for the CXe-CPE electrode exhibit a well-defined pair of peaks attributed to the redox process, demonstrating the presence of Bi^{3+} in the doped xerogels in the composite matrix. Also, the background current can be seen to be higher for the BiCXe-CPE electrode than for the CXe-CPE electrode, which demonstrates the conductive properties of the BiCXe-CPE host matrix, or they may be due to important differences between the porosities of the two materials [Fort CI et al., 2013].

The redox behavior of BiCXe-CPE is a quasi-reversible process that at $v = 50$, V / s is placed at the potential of -0.05 V vs. Ag / AgCl, KCl_{sat} (oxidation), and -0.58 vs. Ag / AgCl, KCl_{sat} (reduction), with a peak separation (ΔE), defined as the difference between the anode and cathode peak potential) of 0.53 V and the ratio between the anode peak and the cathode peak $I_{pa} / I_{pc} = 1.78$. A similar redox behavior of BiCXe-CPE was also observed for square wave voltamograms, where anodic oxidation can be observed much better, oxidation of the bismuth peak being placed at the potential of -0.12 V vs. Ag / AgCl, KCl_{sat}, (Figure 3.7B).

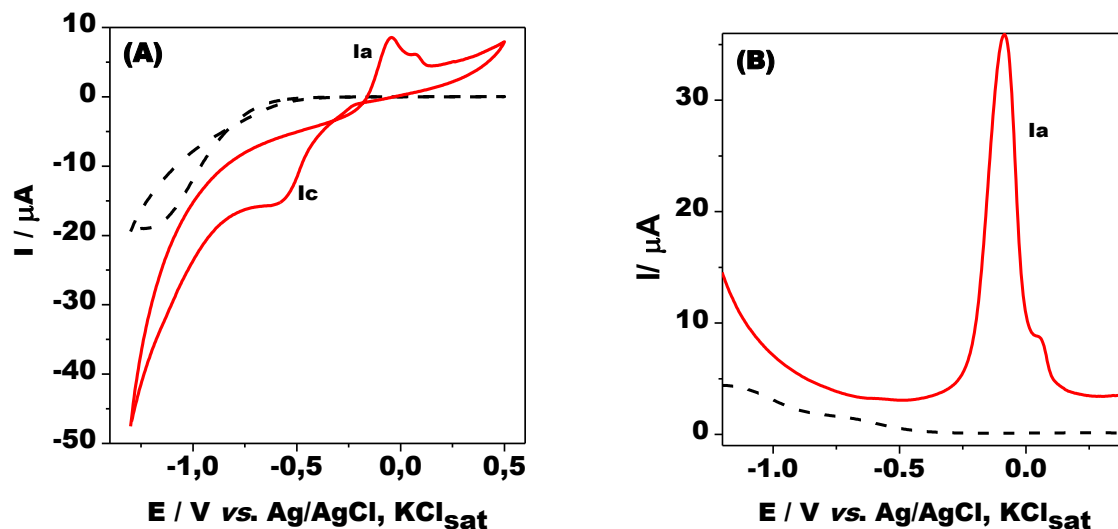


Figure 3.7. Cyclic (A) and square wave voltamograms (B) for CXe-CPE (interrupted line) and BiCXe-CPE (continuous line). Experimental conditions: electrolyte, 0.1 M acetate buffer (pH 4.5); frequency, 25 Hz; amplitude, 0.05 V; potential step, 0.004 V; potential start, -1.2 V; balancing, 10 seconds without shaking.

3.3.3. Cd^{2+} ions detection with BiCXe-CPE

Further, the BiCXe-CPE electrode was examined, recording SWASVs in the presence of Cd^{2+} ions (Figure 3.9). Recorded voltamograms present a well-defined undistorted signal for both Cd^{2+} and Bi^{3+} specific peaks, potentials placed at -0.750 V and -0.12 V vs Ag / AgCl, KCl_{sat} respectively; these values are in line with those reported by other authors [Hocevar S.B. et al., 2005]. With the increase of the concentration of Cd^{2+} ions at 20 μM , the potential peaks specific for Cd^{2+} and Bi^{3+} are shifted to more positive values, -0.665 V ($\Delta E = 0.085$ V) and -0.063 V vs. Ag / AgCl, 0.039 V). The influence of the deposition time of 2 μM Cd^{2+} between 30-360 s on the current response was studied. In the detail of Figure 3.9 we can observe a linear dependence of the current intensity on the deposition time, with the slope of $1.6 \cdot 10^{-2} \pm 0.02 \cdot 10^{-2} \mu\text{A/s}$ ($R = 0.9994$, $n = 7$). Therefore, a metal deposition time of 120 s was chosen, compromised between the sensitivity and the total duration of the experiment.

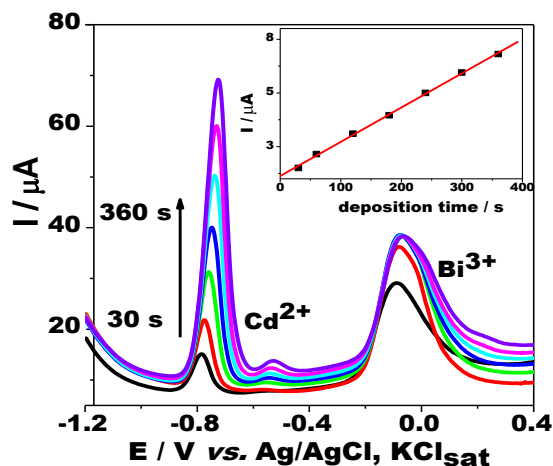


Figure 3.9. SWASVs for 20 μM Cd^{2+} using the BiCXe-CPE electrode for different deposition times. In detail, we can see the dependence of the current on the pic of the deposition time. Experimental conditions: electrolyte, 0.1 M acetate buffer (pH 4.5); frequency, 25 Hz; amplitude, 0.05 V; potential step, 0.004 V; starting potential, -1.2 V; deposition potential -1.2 V; deposition time, 30 s to 360 s with continuous stirring at 500 rpm; balancing, 10 seconds without shaking; electrode conditioning (potential for cleaning), +0.3 V; duration, 30 seconds under continuous stirring conditions at 500 rpm

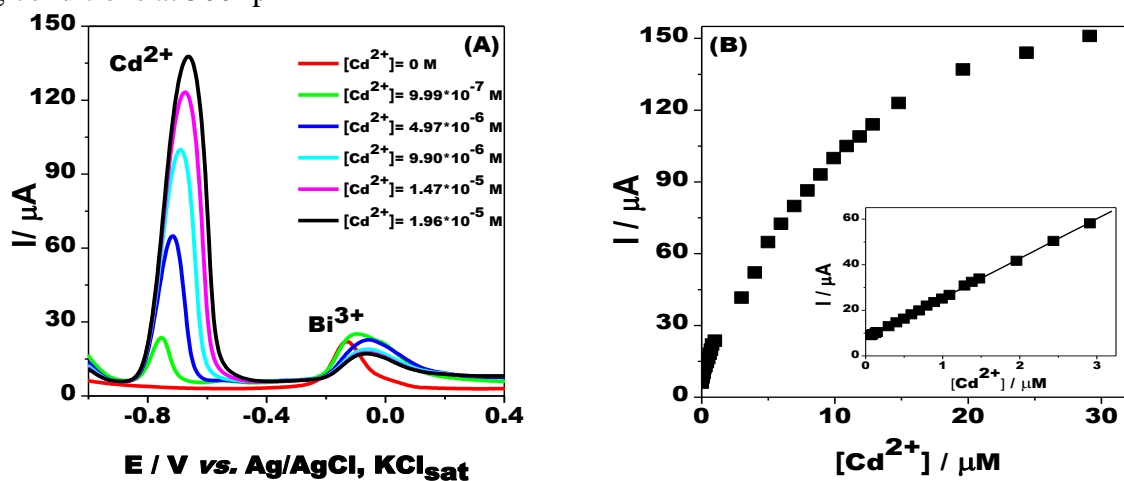


Figure 3.10. SWASVs recorded with BiXe-CPE for detection of Cd^{2+} ions (A) and the corresponding calibration curve (B). Experimental conditions: see Figure 3.9.

Detection of Cd^{2+} ions recorded by SWASVs in the 0-30 μM Cd^{2+} range (Figure 3.10) allows a corresponding calibration curve to be obtained (Figure 3.10 B). The linear range is 0-3 μM Cd^{2+} (Figure 3.10 B in detail) with a slope of $17.39 \pm 0.07 \text{ A} / \text{M}$ ($R = 0.99983$, $n = 21$ points). The detection limit obtained (LOD) was $0.045 \mu\text{M} / \text{L}$ (or $5 \mu\text{g} / \text{L}$) (signal / noise ratio = 3). The LOD value is below the

maximum allowable level of contaminant in drinking water, required and required by EU and US legislation [Council Directive 98/83 / EC of 3 November 1998].

One of the most important performance characteristics of this sensor is reproducibility, expressed as standard deviation (RSD) of peak current or peak potential. In the case of 3 successive measurements for 2 μM Cd^{2+} with BiCXe-CPE in 0.1 M acetate buffer pH 4.5, the mean peak intensity is $2.66 \cdot 10^{-5} \pm 8.38 \cdot 10^{-8}$ A, with a RSD of 0.31%, respectively the peak potential -0.753 ± 0.006 V vs Ag / AgCl, KCl_{sat}, with an RSD of 0.8%. The obtained RSD values indicate good reproducibility of the manufactured sensor, recommending the BiCXe-CPE electrode as a sensor for Cd^{2+} detection.

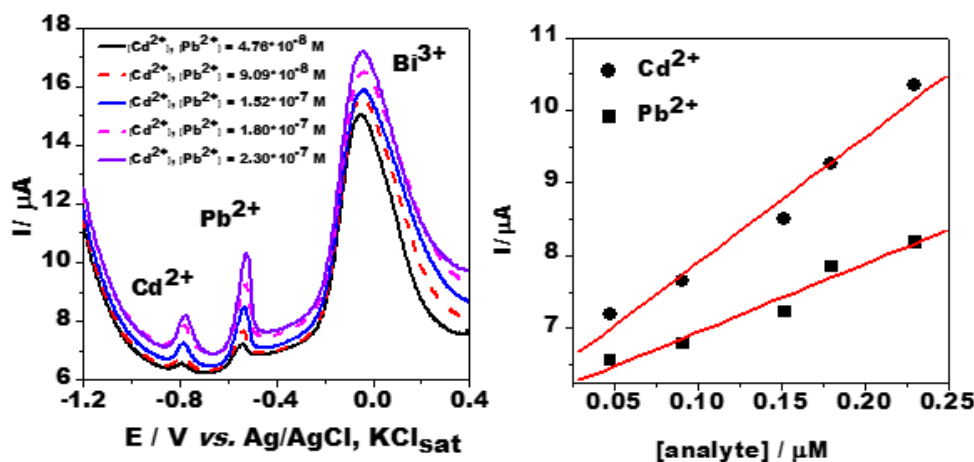


Figure 3.12. SWASVs for increasing concentrations of Cd^{2+} and Pb^{2+} (A) and the corresponding calibration curves (B) for the BiCXe-CPE electrode. Experimental conditions: start potential, -1.3 V vs. Ag / AgCl, KCl_{sat}; deposition time 120 s with continuous stirring; other conditions: see figure 3.9.

From the calibration curves for Cd^{2+} and Pb^{2+} ions (Figure 3.12 B), the calculated sensitivities are: 9.36 ± 1.13 A / M for Cd^{2+} ($R = 0.980$, $n = 5$) and 17.31 ± 1.68 A / M for Pb^{2+} ($n = 5$). The BiCXe-CPE electrode was selective enough to detect Pb^{2+} ions, so it can be applied not only in the individual determination of Cd^{2+} ions but also in the simultaneous determination of Cd^{2+} and Pb^{2+} ions [Deac A.R. et al., 2015].

3.3.5. Detection of Pb^{2+} ions with the BiCXe-CPE

As expected, the peak current attributed to the Pb^{2+} ions increases linearly when the deposition potential is increased from -0.9 to -1.4 V vs. Ag / AgCl, KCl_{sat}, as shown in Figure 3.13 B, respecting a dependency described by the equation: $I/A = (10.7 \cdot 10^{-6} \pm 1.8 \cdot 10^{-6}) - (25.5 \cdot 10^{-6} \pm 1.53 \cdot 10^{-6}) E_{\text{dep}}/V$, $R =$

0.9929, $n = 6$. To obtain a peak with maximum intensity in the detection of Pb^{2+} ions, a deposition potential of -1.3 V vs. $\text{Ag} / \text{AgCl}, \text{KCl}_{\text{sat}}$ in the next experiments.

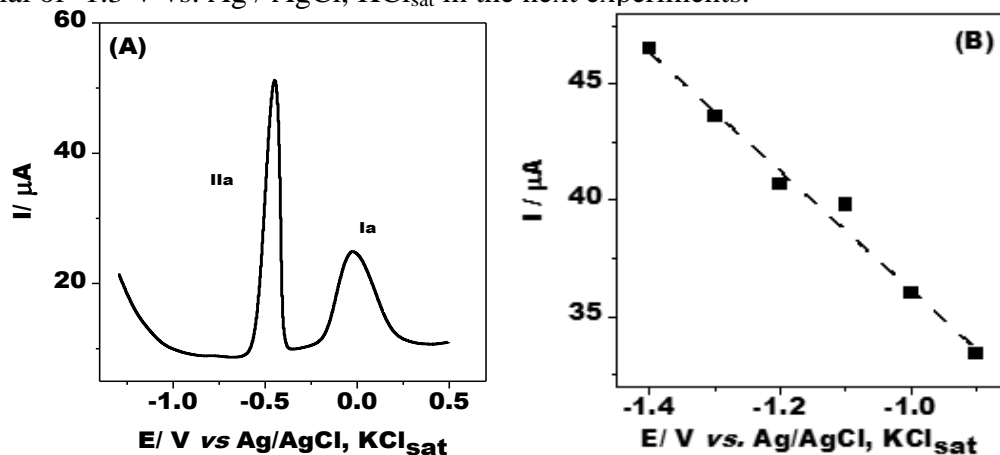


Figure 3.13 SWASV for the detection of Pb^{2+} ions with the BiCXe-CPE electrode (A) and the deposition potential influence for the detection of $2 \mu\text{M}$ Pb^{2+} with the BiCXe-CPE electrode by SWASVs (B). Experimental conditions: electrolyte, 0.1 M acetate buffer ($\text{pH} 4.5$); potential start, -1.3 V vs. $\text{Ag} / \text{AgCl}, \text{KCl}_{\text{sat}}$; frequency, 25 Hz ; amplitude, 0.05 V ; potential step, 0.004 V ; potential deposit -0.9 to -1.4 V vs. $\text{Ag} / \text{AgCl}, \text{KCl}_{\text{sat}}$, deposition time, 120 s with continuous stirring at 500 rpm ; balancing, 10 seconds without shaking; electrode conditioning, $+0.3 \text{ V}$ vs. $\text{Ag} / \text{AgCl}, \text{KCl}_{\text{sat}}$, duration, 30 seconds with continuous stirring at 500 rpm

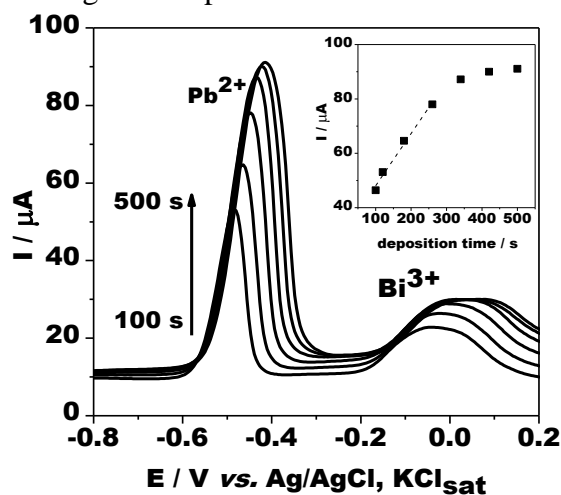


Figure 3.14. The influence of accumulation time on SWASV detection of $2 \mu\text{M}$ Pb^{2+} with the BiCXe-CPE electrode. In detail: Dependence of the peak current intensity of Pb^{2+} vs. deposition time. Experimental conditions: see fig 3.13.

As can be seen in Figure 3.14, a linear dependence of the peak current at accumulation time intervals of less than 200 seconds with a slope value of $200 \text{ nA} / \text{s}$ ($R = 0.999$, $n = 5$) is shown,

demonstrating a higher selectivity than that obtained with silver electrodes made from a recordable compact disc (ACD), for which a slope of 180 nA / s (R2 = 0.998) was reported [Honeychurch KC, 2013]. If an accumulation time of more than 200 s is applied, a gradual leveling of 500 μs of peak current due to the saturation occurring at the electrode surface is observed [Li D. et al., 2010].

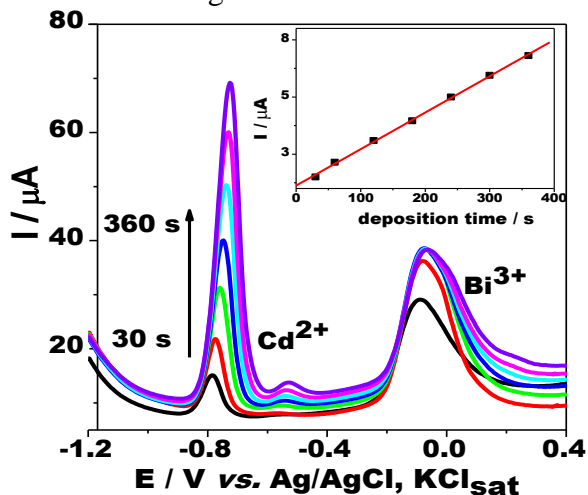


Figure 3.15 SWASVs for determination of Pb^{2+} ions with the BiCXe-CPE (A) electrode and the corresponding calibration curve (B). Experimental conditions: electrolyte, 0.1 M acetate buffer (pH 4); potential start, -1.3 V vs. Ag / AgCl, KCl_{sat}; frequency, 25 Hz; amplitude, 0.05 V; potential step, 0.004 V; potential deposit -1.3 V vs. Ag / AgCl, KCl_{sat}; deposit time, 120 s with continuous stirring at 500 rpm; balancing, 10 seconds without shaking; electrode conditioning, + 0.3 V vs. Ag / AgCl, KCl_{sat}, duration, 20 s under agitation conditions at 500 rpm

Table 3.1 Analytical parameters for detection of Pb^{2+} ions with BiCXe-CPE. Experimental conditions: see figure 3.15

Linear domain Nm	Sensibility A/M	LOD M	LOD μg/l	R/n
$2 \cdot 10^{-9} \div 5 \cdot 10^{-9}$	453.06 ± 59.96	$8.81 \cdot 10^{-10}$	0.18	0.9829 /6
$5 \cdot 10^{-9} \div 2.5 \cdot 10^{-8}$	49.66 ± 4.63	$4.28 \cdot 10^{-9}$	0.88	0.9872 /5
$2.5 \cdot 10^{-8} \div 3.5 \cdot 10^{-7}$	37.95 ± 1.56	$4.12 \cdot 10^{-8}$	8.55	0.9933/10

* LOD is calculated with formula $3 \cdot \text{SD} / \text{slope}$; slope equation $I / \text{A} = a + b [\text{Pb}^{2+}] / \text{M}$

The SWASV voltamograms recorded for different concentrations of Pb^{2+} metal ions under the optimal experimental conditions have a well-defined peak shape, corresponding to the oxidation of Pb (0) accumulated on the surface of the BiCXe-CPE electrode (Figure 3.15 A). The resulting calibration curve has a linear range between $2 \cdot 10^{-9}$ și $5 \cdot 10^{-9}$ M Pb^{2+} , described by the equation $I/A = (1.54 \cdot 10^{-5} \pm 2.19 \cdot 10^{-7}) + (453.06 \pm 59.96) [Pb^{2+}]/M$ ($R = 0.9829$, $n = 6$) (Figure 3.15 B and detail).

The estimated detection limit for the signal / noise ratio = 3 was $0.18 \mu\text{g/l } Pb^{2+}$. This value is much lower than $1.3 \mu\text{g/l } Pb^{2+}$, a value obtained for a similar electrode, more precisely a glassy carbon electrode modified with bismuth-based carbon black and Nafion (GC / Bi-xerogel / Nafion) used by Dimovasilis and Prodromidis [Dimovasilis PA, Prodromidis MI, 2013].

Capitolul 4. Screen printed electrodes based on carbon xerogels doped with Bi^{3+}

This part of the paper is intended for experiments focused on creating an ink that can be used in the preparation of screen-printed electrodes.

4.2. Ink characterization

In order to study the characteristics of prepared solutions for printing, several samples of various compositions are presented in table 4.2

Table 4.2. The solutions analyzed and the concentrations used

Sample	Conc (C-Bi) _{CS}	Conc TX-100	Conc IPA	H ₂ O
IK4	0,0021 g / 0,05%	4,10 ml / 36,95%	4,29 ml / 27%	4,5 ml / 36%
IK8	0,012 g / 0,1%	2,69 ml / 24%	5,25 ml / 33%	5,25 ml / 42,9%
IK9	0,0125 g / 0,1%	1,40 ml / 12,9%	5,88 ml / 37%	6,25 ml / 50%
IK11	0,012 g / 0,1%	2,34 ml / 23,3%	5,25 ml / 34,6%	5,37 ml / 42%

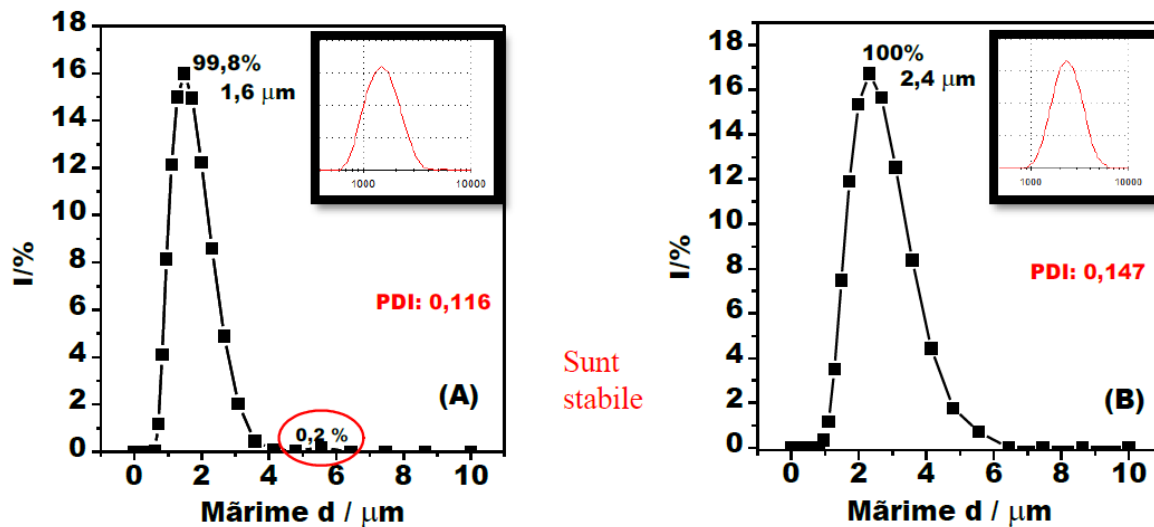


Table 4.3. Systems classification by the degree of particle dispersion

Systems	monodisperse		polydisperse
Tip	Uniform	Narrow	Large
PDI	0.0	0.0-0.1	> 0.4

As can be seen from figure 4.4 the PDI index of both tested solutions has a value of 0.1. In the case of the first system, IK 11 analyzed in the first minute, a slight sedimentation of 0.2% appears in which particle sizes vary between 4.5 and 6 μm . This is a characteristic, apparently, for the systems analyzed in the first minute after manufacturing the solution; this detail was also observed in the IK 9 system (Figure 4.3); instead, this solution is quite stable.

In case of solution IK8, solution analyzed after 24 hours, it is found that it has the characteristics that allow the following steps to be taken for the manufacture of a screen printed electrode.

To express a correct viscosity value, three consecutive measurements were made for the same solution. The following viscosity values were obtained: $\eta = 10 \text{ mPa}\cdot\text{s}$, $\eta = 9,66 \text{ mPa}$, $\eta = 9,69 \text{ mPa}\cdot\text{s}$. The final value was calculated by the arithmetic mean of the three measurements; the average viscosity being 9.78 mPa.s.

To begin with, ink with the characteristics considered to be the best was manual printed on photographic paper. Following the scotch tests, the adhesion of the solution to photographic paper proved to be good.



Figure 4.11. Manual screen printing on photographic paper

Capitolul 5. Electrodes modified based on hemin for H₂O₂ detection

In this context, one of the objectives of the thesis was to obtain electrodes modified with hemin, having high stability. Increased stability has been achieved in two ways:

- By electrochemical polymerization of hemin on the electrode, simultaneously with the reduction of graphene oxide;
- By incorporating hemin into melamine dendrimer.

The results of the research are presented below.

5.1. Modified electrode based on oxid graphene and hemin

5.1.1. Modified electrode preparation

A stock solution of GO / TRIS was prepared by dissolving 10 mg of solid material in 10 ml of 0.05 M TRIS solution. A 0.5 mM Hm solution was also prepared by dissolving an appropriate amount of hemin in a 0.05 M TRIS solution. Prior to modified the work electrode, its surface was cleaned by grinding on abrasive paper with distilled water and ultrasonic for 30 minutes in distilled water.

Modification of the G / rGO / polyHm electrode involves a two-step procedure: *drop-casting* and electrochemical modification. *Drop casting* consists of depositing on the surface of the graphite electrode 5 μ L suspension of GO / TRIS, dried with hot air flow. The second step consists in cycling the electrode in the potential range between +0.2 and -1.0 V vs. Ag / AgCl, KCl_{sat} in 0.5 mM Hm solution. This process simultaneously produces the reduction of graphene oxide and the

formation of polymerized hemin-layers. The goal was to obtain a stable redox matrix. After this modification, the working electrode was used without any other chemical or electrochemical treatment.

5.1.2. Modified electrodes characterization

Electrochemical characterization of electrodes

The pair of peaks very well defined from the voltammograms presented in figure 5.3 (A1 / C1) was associated with the quasi-reversible monoelectronic transfer between the (Fe³⁺) / (Fe²⁺) redox couple present inside the hemin, according to equation 5.1:

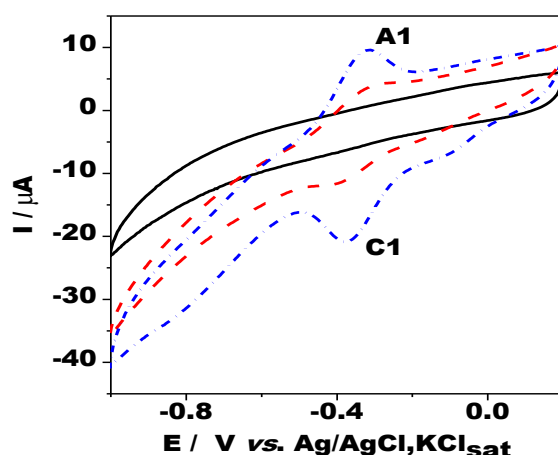
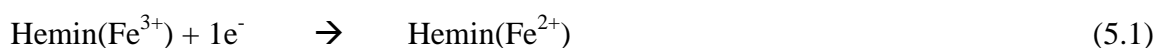


Figure 5.3. Cyclic voltammograms for electrodes G (continuous line, black), G / polyHm (broken line, red) and G / rGO / polyHm (dotted line, blue). Experimental conditions: electrolyte, 0.1 M phosphate buffer (pH 7); scan rate, 0.050 V s⁻¹; potential start, +0.2 vs. vs. Ag / AgCl, KCl_{sat}; electrode preparation by electropolymerization: electrolyte, 0.05 mM Hm in 0.5 M TRIS; scan rate, 0.025 V s⁻¹, 30 cycles

In order to optimize the production of the modified G / rGO / polyHm electrode, the hemin electropolymerization was performed at different scan rates (0.010, 0.025 and 0.100 V s⁻¹), performing 30 or 50 cycles between 0.2 V and -1.0 V vs. Ag / AgCl, KCl_{sat}, in 0.5 mM Hm in 0.05 M TRIS-Cl (pH 8), the electrode thus modified was then tested in phosphate buffer (pH 7). As can be seen in figure 5.4. A, peak current intensities reach the maximum for both anodic and cathodic processes at 2.700 s, which means a scan rate of 0.025 mV s⁻¹ for 30 cycles. Some authors limit the increase in thickness of

the polymerised hemin film by applying 10-20 cycles to 0.1 V s^{-1} . The low sweep rate applied in our case provides the time required for simultaneous reduction of graphene oxide and hemin polymerization.

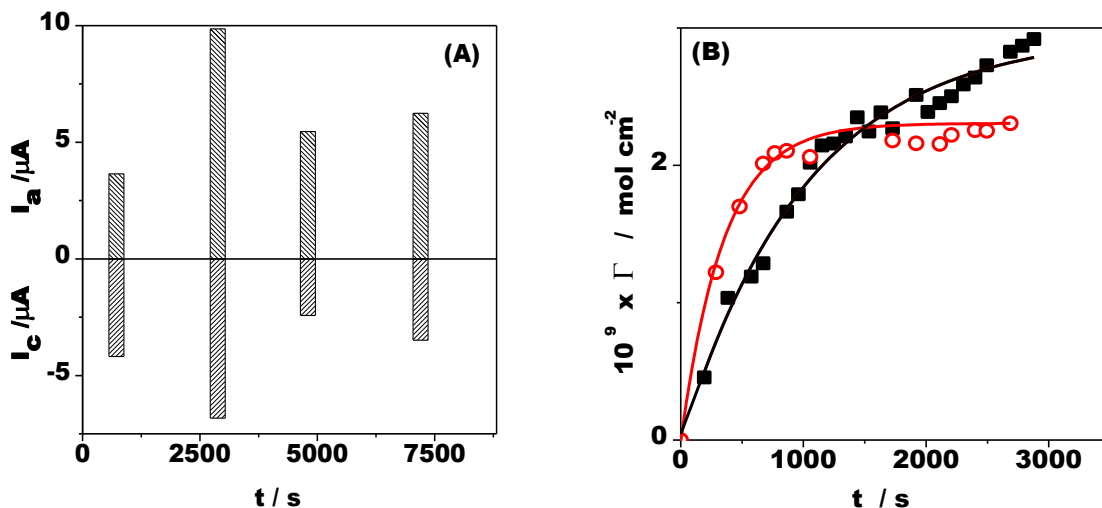


Figure 5.4. . The influence of the electropolymerization time (t) on the current intensity for the G / rGO / polyHm electrode tested in phosphate buffer (A) and the variation of the superficial concentration of the polymerized hemin Γ , with the time of obtaining the film of polyhemin on electrodes, G/polyHm (●) and G/rGO/polyHm (■) in the phosphate buffer solution (B). Experimental conditions: (A) electropolymerization: electrolyte, 0.05 mM Hm in 0.5 M TRIS; scan rate, 0.010, 0.025 and 0.1 V s^{-1} during 30 or 50 cycles; electrode testing: electrolyte, 0.1 M phosphate buffer (pH 7); scan rate 0.05 V s^{-1} ; potential start, +0.2 vs. Ag / AgCl, KCl_{sat} ; (B) electrode preparation by electropolymerization: electrolyte, 0.05 mM Hm in 0.5 M TRIS; scan rate, 0.025 V s^{-1} , 30 cycles

According to the study conducted to test the influence of the scan rate, it was concluded that no matter what value is used to obtain the modified electrodes, the values of the slopes of the $\log I - \log v$ close to 1 show a good immobilization of polyhemin on the surface of the electrode in the presence of rGO.

Table 5.1. Dependence I versus scan rate. Experimental conditions: see figure 5.

Electrode type	slope log I vs v R/n	
	Anodic	catodic
G/polyHm (0,025 V/s)	$\frac{0.760 \pm 0.016}{0.9980/11}$	$\frac{1.007 \pm 0.039}{0.9933/11}$
G/rGO/polyHm (0,025 V/s)	$\frac{0.884 \pm 0.011}{0.9993/11}$	$\frac{1.567 \pm 0.118}{0.9754/11}$
G/polyHm (0,1V/s)	$\frac{0.868 \pm 0.016}{0.9980/14}$	$\frac{0.831 \pm 0.014}{0.9983/14}$
G/rGO/polyHm (0,1 V/s)	$\frac{0.914 \pm 0.024}{0.99572/14}$	$\frac{0.918 \pm 0.022}{0.9964/14}$

The polyhemin stability adsorbed on the G / rGO / polyHm electrode was investigated under potentiodynamic conditions by recording successive cyclic voltamograms in 0.1M phosphate buffer (pH 7) in the absence and presence of 0.025 mM H₂O₂. From a qualitative point of view, recorded voltamograms remain practically unchanged.

5.1.3. Determination of H₂O₂ with modified electrodes G / rGO / poly Hm

5.1.3.1. Determination of H₂O₂ concentration in a real sample

Under optimized experimental conditions, in order to prove the possibility of using the G / rGO / polyHm electrode for the analysis of real samples, the H₂O₂ detection from a commercial pharmaceutical product was performed by the standard addition method.

With the G / rGO / polyHm electrode, a concentration of 0.165 mM H₂O₂ was estimated for the unknown pharmaceutical sample. This value is in very good concordance with the concentration indicated by the manufacturer (0.170 mM).

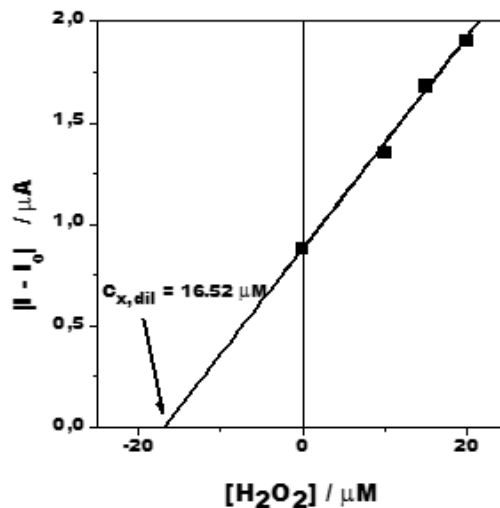


Figure 5.10 Curve representation for standard addition method for G / rGO / polyHm electrode in H₂O₂ detection of pharmaceutical disinfectant solution by square wave voltammetry. Experimental conditions: an injection of the actual diluted sample, followed by 3 injections of a standard solution of 10⁻² M H₂O₂; for other conditions figure 5.9.

5.3.1. Electrodes modified with melaminic compounds and hemin

Another way to increase the stability and efficiency of hemin-modified electrodes is to incorporate hemin into an organic matrix.

5.3.2. Preparation of modified electrode

10⁻³ M stock solutions for Dim, Den and Hm were individually prepared by dissolving them in DMSO. Standard solutions of 5 mM Hm-Dim and Hm-Den were prepared by dissolving the corresponding amount of hemin in the stock solutions of the melamine compounds. The surface of the glassy carbon electrode was then modified by depositing 10 μL of the above mentioned homogeneous mixtures and subjected to a hot air treatment to evaporate the solvent. The electrode thus obtained was ready for use without further chemical or electrochemical procedures being required.

Vibrational analyzes, FT-IR, show intramolecular interactions in solid state, between hemin molecules and melamine compounds, Dim and Den respectively. These interactions can be grouped into: intramolecular interactions between H-bonds, proton inter-shifts and π-π interactions.

5.3.3.2. Electrochemical methods

In the absence of hemin (Hm), no redox process is observed. The presence of the hemin on the electrode causes the clear appearance of a pair of peaks, which can be attributed to the Fe (II) / Fe (III) redox couple existing in the hemin molecule.

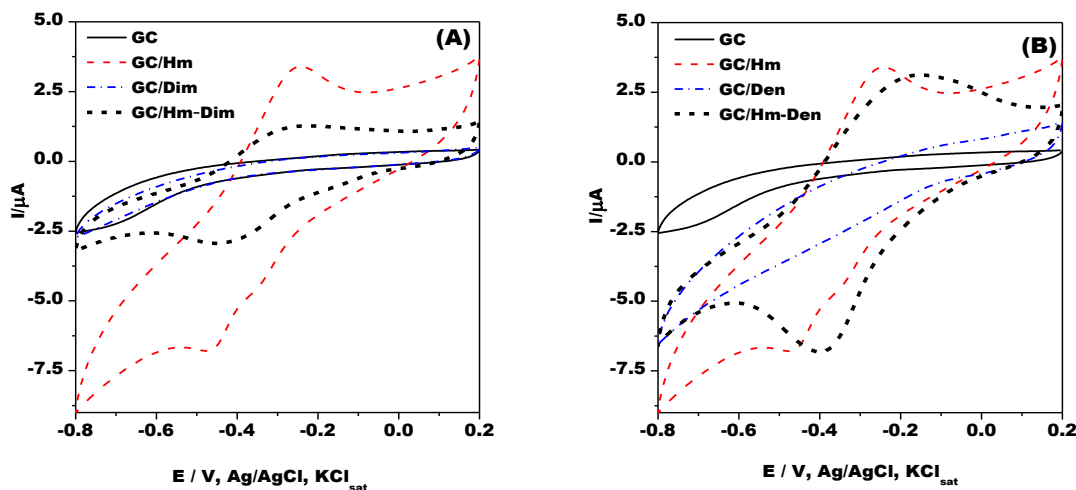


Figure 5.13. (A) Cyclic voltammograms for GC, GC-Hm, GC / Dim, GC / Hm-Dim and (B) cyclic voltammograms for GC, GC-Hm, GC / Den, GC / Hm -Den. Experimental conditions: electrolyte, 0.1 M, phosphate buffer (pH 7); scan rate, 50 mV s⁻¹; potential start, 0.2 V

From table 5.4 we can see the degree of electrode surface coverage that is higher than that corresponding to the mono-layer of heme ($7.5 \times 10^{-11} \text{ m}^2 \text{ cm}^{-2}$) presented by Brusova and Magner [Brusova Z., Magner E., 2009], indicating the formation of more than one hemin monolayer.

For both GC / Hm-Dim and GC / Hm-Den electrodes, the voltammogram form remains invariant during cycling, demonstrating good stability and only a small variation in concentration on the surface of the electrode, as shown also in figure 5.15 for the electrode GC / Hm-Den. The current of the 50th cycle represents 84% of the anode peak current and 95% of the cathode current of the first cycle.

Electrochemical Impedance Measurements (EIS)

In order to determine the activity of modified electrodes, Nyquist impedance diagrams were recorded in the presence of the $[\text{Fe}(\text{CN})_6]^{3-} - [\text{Fe}(\text{CN})_6]^{4-}$ solution (figure 5.16). It can be noticed that the system exhibits diffusion dominated behavior at low frequencies. Unsurprisingly, the presence of Dim and Den compounds on the surface of the electrode brings a significant

increase in the imaginary impedance component, suggesting that melamine adsorbed to the surface of the electrode impedes access to the redox couple $[\text{Fe}(\text{CN})_6]^{3-} - [\text{Fe}(\text{CN})_6]^{4-}$ to the electrode; due to low conductivity, adsorbed hemina also contributes to impedance increase, an idea supported by Laviron in 1979 [Laviron E., 1979].

Table 5.4. Electrochemical parameters of the voltammetric response for modified GC / Hm, GC / Hm-Dim and GC / Hm-Den electrodes. Experimental conditions: see figure 5.14.

Electrod	ΔE_p (V)	E_{FWHM} (V)		E^0 (V/Ag/AgCl/KCl)	Ia/Ic	Surface coverage* (mol cm ⁻²)	
		anodic	catodic			anodic	catodic
GC/Hm	0.194	0.218	0.173	-0.358	-1.948	$2.33 \cdot 10^{-9}$	$8.51 \cdot 10^{-10}$
GC/Hm-Dim	0.140	0.169	0.128	-0.349	1.189	$1.27 \cdot 10^{-9}$	$7.66 \cdot 10^{-10}$
GC/Hm-Den	0.177	0.117	0.210	-0.271	0.933	$3.21 \cdot 10^{-9}$	$2.30 \cdot 10^{-9}$

*calculated with equation: $\Gamma = \frac{Q}{(zFA v)}$ where Q= área under the pic (in C) recored between the VOC masurements (50 mV)

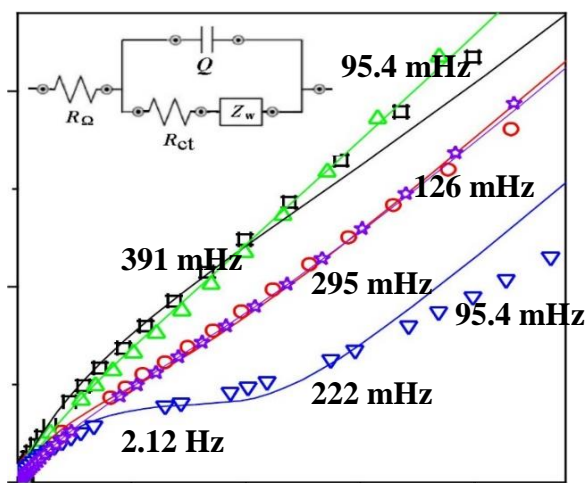


Figure 5.16 The Nyquist impedance spectra for modified electrodes GC (\square), GC / Dim (\circ), GC / Hm-Dim (\triangle), GC / Den (∇) and GC / Hm-Den (\star) recorded in the open circuit after immersion in the 0.1 M KCl + 0.05 mM $[\text{Fe}(\text{CN})_6]^{3-}/[\text{Fe}(\text{CN})_6]^{4-}$ (In detail: equivalent electric circuit $R_r(Q(R_{ct}W))$), used for modeling modified or unmodified electrodes)

5.3.4. Amperometric detection of H₂O₂

In order to verify the electrocatalytic activity of GC / Hm-Dim and GC / Hm-Den electrodes towards to H₂O₂ reduction, their electrochemical response was recorded in the absence and presence of 5x10⁻⁵ M H₂O₂ (Figure 5.17).

A significant increase in cathode peak current at GC / Hm-Dim and GC / Hm-Den electrodes is observed compared to GC and CG / Dim or CG / Den electrodes, demonstrating the electrocatalytic effect of modified electrodes.

The catalytic efficiency of the modified electrodes (calculated as CE (%) = (I_{pc, H₂O₂} - I_{pc, 0}) / I_{pc, 0} where: I_{pc, 0} is the current of the cathode peak recorded in the absence of H₂O₂ and I_{pc, H₂O₂} is the current of the cathode peak recorded in the presence of H₂O₂) was 77.66% for GC / Hm-Dim and 64.98% for GC / Hm-Den. The magnitude of these values indicates that hemin, like peroxidase, has a good catalytic intrinsic activity, which can facilitate the reduction of H₂O₂.

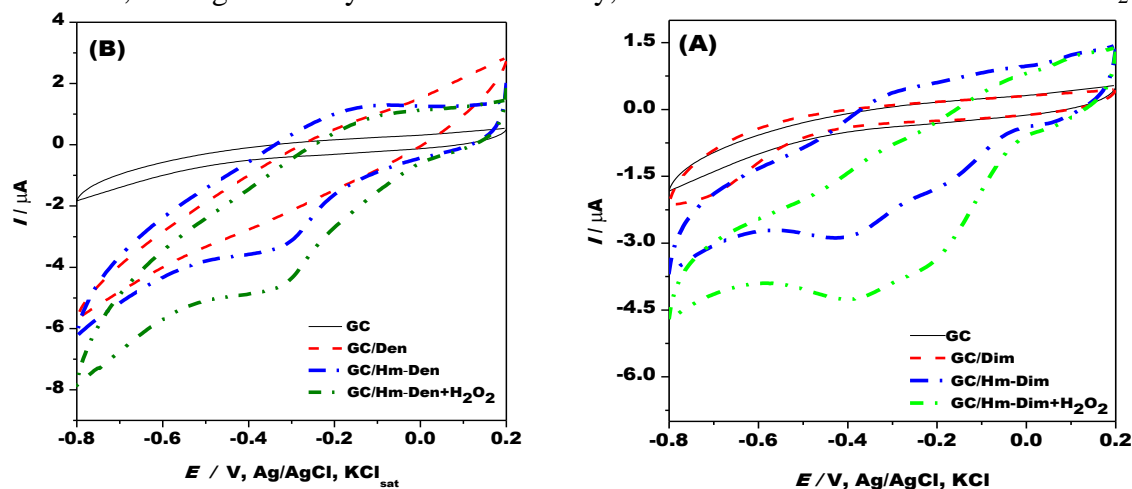


Figure 5.17 Cyclic voltammograms in the presence of 0.05 mM H₂O₂ for electrodes GC (A, B, continuous line), GC / Dim (A, broken line), GC / Den (B, 2-point line) and GC / Hm-Den (B) electrodes in the absence of H₂O₂. Experimental conditions: electrolyte, 0.1 M, phosphate buffer (pH 7); scan rate, 50 mV s⁻¹; potential start, 0.2 V vs. Ag / AgCl, KCl_{sat}

Amperometry

Figure 5.18. presents the typical calibration curves obtained with different electrodes, applying a constant potential of -0.35 V vs. Ag / AgCl, KCl_{sat} and adding successive concentrations of H₂O₂. Analytical parameters values show that the presence of hemin in the composite matrix on the surface of the electrode improves the sensitivity and decreases the detection limit for H₂O₂, as

compared to unmodified electrodes. The best electroanalytic parameters were obtained for the GC / Hm-Dim electrode, probably because of the more convenient steric orientation of the heme units on the electrode surface, allowing a good communication between the redox centers and the glassy carbon substrate.

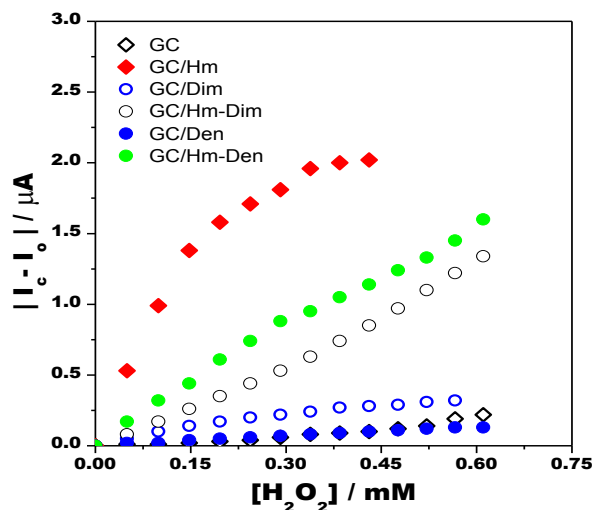
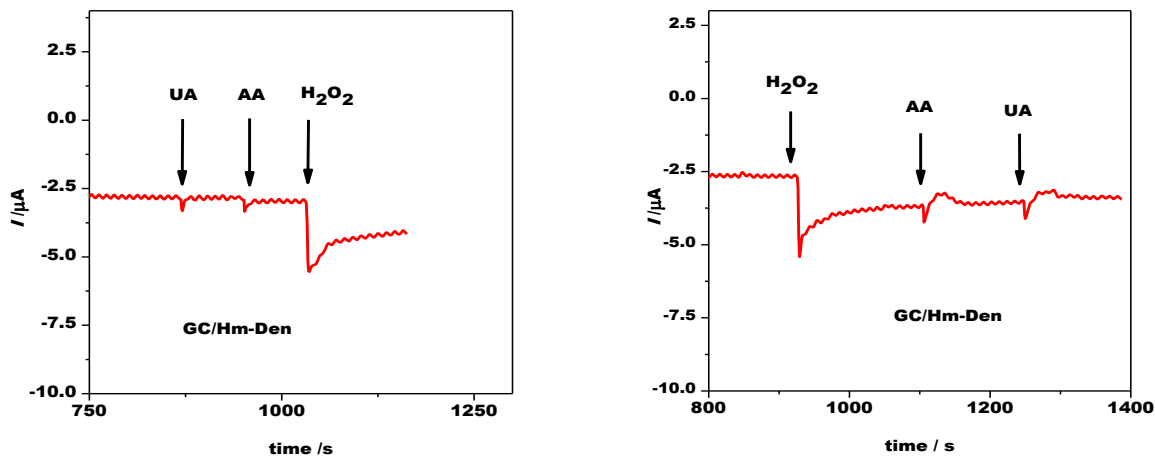


Figure 5.18. Calibration curves for H_2O_2 detection with GC (A, B), GC / Hm (A, B), GC / Dim (A), GC / Den (B) Hm-Den (B. Successive additions of different H_2O_2 concentrations) Experimental conditions: electrolyte, 0.1 M phosphate buffer (pH 7), applied potential, -0.35 V vs. Ag / AgCl, KCl_{sat} , 2 M continuous stirring

With regard to electrode selectivity, the amperometric responses recorded after the addition of 500 μL of 10^{-2} M uric acid and ascorbic acid solution and 500 μL of 10^{-2} M H_2O_2 concentration in 10 mL of buffer, at an applied potential of -0.35 V vs Ag / AgCl / KCl_{sat} . the resulting amperograms do not show any variation in the H_2O_2 current intensity (figure 5.18).



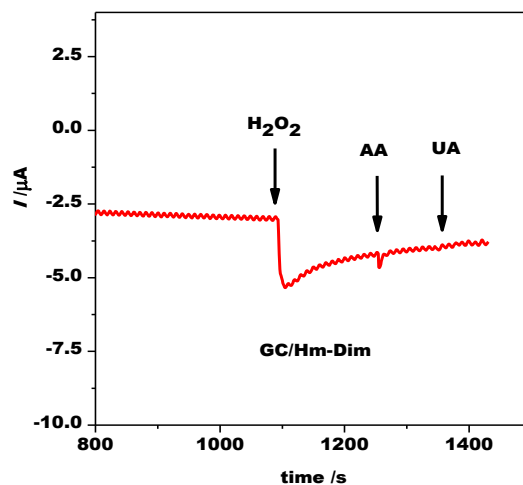


Figure 5.18. The amperometric response of modified GC / Hm-Dim and GC / Hm-Den electrodes in the presence of successive addition of H₂O₂, uric acid (UA) and ascorbic acid (AA). Experimental conditions: electrolyte, 0.1 M, phosphate buffer (pH 7), final concentration 0.5 mM analyte stock solutions 10⁻² M; potentially applied, -0.35 V vs. Ag / AgCl / KCl sat

General Conclusions and Perspectives

1. New composite nanomaterials based on carbon xerogels and bismuth were prepared by a sol-gel method for their use as electrode materials for the detection of Cd²⁺ and Pb²⁺ metal ions
3. The linear range of modified electrodes (BiCXe-CPE) in the detection of Cd²⁺, Pb²⁺ heavy metal ions is 10⁻⁸-10⁻⁵M or 10⁻¹⁰-10⁻⁵M, the detection limit being 10⁻⁸M Cd²⁺ 10⁻¹⁰ M Pb²⁺, respectively. These performances recommend the BiCXe-CPE electrode for detecting Cd²⁺, and Pb²⁺ ions from real samples.
4. A Bi-modified xerogel C-based conductive ink was developed and characterized to produce modified screen printed electrodes used for the detection of heavy metals.
5. Two new types of hemin-modified electrodes were prepared and characterized by morpho structural (SEM, FT-IR, XRD) and electrochemical (cyclic voltammetry, electrochemical impedance spectroscopy) methods:
 - A graphite electrode modified with polyhemin and graphene oxide, prepared by simultaneous electrochemical reduction of graphene oxide (GO) and electropolymerization of hemin;
 - A modified glassy carbon with hemin and two new melamine compounds synthesized in the faculty's organic chemistry department: a G-0 dimer and a G-2 dendrimer (2,4,6-triamino-1,3,5-triazine) .

7. The newly prepared electrodes were successfully tested in the H₂O₂ detection process (for the GC / Hm-Dim electrode, the catalytic efficiency was 77.66% and for GC / Hm-Den 64.98%; for the G / polyHm electrode tested in phosphate buffer the detection limit was 13.3 μM, compared to the value obtained with the G / rGO / polyHm electrode of 8.88 μM).

Selective bibliography

45. **Deac A.R.**, Coteț L.C., Turdean G.L., Mureșan L.M., Carbon paste electrode modified with Bi³⁺- impregnated carbon xerogel for Pb²⁺ determination by square wave anodic stripping voltammetry, *Revue Roumaine de Chimie*, 60(7-8), pag 697-705, 2015 a.
46. **Deac A.R.**, Coteț L.C., Turdean G.L., Mureșan L.M., Determination of Cd(II) using square wave anodic stripping voltammetry at a carbon paste electrode containing Bi- impregnated carbon xerogel, *Studia Univ. Babeș Bolyai Chem.*,1, 2015 b.
47. **Deac A.R.**, Cristina Morar, Graziella Liana Turdean, Mircea Darabantu, Emese Gal, Liana Maria Muresan, Glassy carbon electrode modified with hemin and new melamine compounds for H₂O₂ amperometric detection, *Journal of solid state electrochemistry*, 2016, p 1-11.
48. **Deac A.R.**, Liana Maria Muresan, Liviu Cosmin Cotet, Lucian Baia, Graziella Liana Turdean, Hybrid composite material based on graphene and polyhemin for electrochemical detection of hydrogen peroxide, *Journal of Electroanalytical Chemistry* 802C, 2017, pp. 40-47
60. Fort C.I., Coteț L.C., Vulpoi A. , Turdean G.L., Danciu V., Baia L., Popescu I.C., Bismuth doped carbon xerogel nanocomposite incorporated in chitosan matrix for ultrasensitive voltammetric detection of Pb(II) and Cd(II), *Sens. Actuators, B*, Vol 220, 2015, pag 712–719.
62. Frelinger S.N., Ledvina M.D., Kyle J.R., Zhao D., *Ore Geology Reviews*, Scanning electron microscopy cathodoluminescence of quartz: Principles, techniques and applications in geology, 65, pag 840-852, 2015.
70. Gu T.T., Wu X.M., Dong Y.M., Wang G.L., Novel photoelectrochemical hydrogen peroxide sensor based on hemin sensitized nanoporous NiO based photocathode, *J. Electroanal. Chem*, 759, pag 27-31, 2015.
79. Hench L.L., West J.K., *The sol-gel process*, *Chem Rev*, 90(1), pag 33–72, 1990.
83. Hotărârea de Guvern nr. 699/2003

84. Hotărârea de Guvern nr. 735/2006

85. H.G. nr 371 din 14.10.2010.

107. Laviron E., The use of linear potential sweep voltammetry and of a.c. voltammetry for the study of the surface electrochemical reaction of strongly adsorbed systems and of redox modified electrodes, *J. Electroanal. Chem. Interfacial Electrochem.*, 100, pag 263-270, 1979.

119. Lindfors T., Österholm A., Kauppila J., Gyurcsányi R.E. , Enhanced electron transfer in composite films of reduced graphene oxide and poly(N-methylaniline), *Carbon Volume 63*, pag 588–592, 2013.

120. Liu L., Song Y., Wang L., Yuan H., Zhang M., Xiang Y., et al., Architecture of DNA–multiwalled carbon nanotubes–silver nanoparticles composites–modified glassy carbon electrode for hydrogen peroxide detection, *Environ. Eng. Sci.*, 29, pag 59–63, 2012

136. Miao X., Yang C., Leung C.H., Ma D.L., Application of iridium(III) complex in label-free and non-enzymatic electrochemical detection of hydrogen peroxide based on a novel “on-off-on” switch platform, *Scientific reports 6*, article number 25774, pag 1-8, 2016.

151. Perez del Pino A., Gyogya E., Coteț L.C., Baia L., Logofatu C., Laser-induced Chemical Transformation of Free-standing Graphene Oxide Membranes in Liquid and Gas Ammonia Environments, *RSC*, 1-3, 2016.

166. Sealy C., Carbon-based membranes fill the gap, *Materials today*, 19 (10), pag 558, 2016.

208. Wang L, Yang H., He J., Zhang Y., Yu J., Song Y., Cu-hemin metal organic frameworks/chitosan reduced graphene oxide nanocomposites with peroxidase like bioactivity for electrochemical sensing, *Electrochim. Acta*, 231, pag 691-697, 2016.

226. Zang P., Shuangyan G., Dang L., Zonghuai L., Zhibin L., Green synthesis of holey graphene sheets and their assembly into aerogel with improved ion transport property, *Electrochim. Acta*, 212(10) pag 171–178, 2016.

228. Zhao G., Yin Y., Wang H., Liu G., Wang Z., Sensitive stripping voltammetric determination of Cd(II) and Pb(II) by a Bi/multi-walled carbon nanotube-emeraldine base polyaniline-Nafion composite modified glassy carbon electrode, *Electrochim. Acta*, 2008, Vol 220, pag 267–275, 2016.

link 19-

Encyclopedia Britannica, visited 29.09.2016- accesat în data de 26.08.2017;